Program for exergy analysis of steel refining in a ladle furnace

David de Souza Zanon [1]
Gabriel Evangelista Medeiros [1]
Sonia Letichevsky [1]
Roberto Ribeiro de Avillez [1*]

Abstract

The optimization of industrial processes is an interesting strategy to mitigate the environmental impact of productive activities. It involves applying multidisciplinary knowledge to improve the efficiency of industrial processes, thereby reducing the consumption of natural resources, pollutant emissions, and material waste. Exergy analysis has been extensively addressed in literature, with numerous studies focused on this topic. The most prevalent research areas include analyzing industrial processes, optimizing energy generation and distribution systems, and assessing energy efficiency in transportation systems and buildings. The literature provides various exergy analysis studies conducted for electric arc furnaces (EAF) used in steel production. However, there is a need for more research focused on applying exergy analysis to the ladle furnace (LF) refining process, which represents the second stage of secondary steel refining in the industry. A Python program using Jupyter Notebook was developed to calculate steel refinement's mass, energy, and exergy balances in a ladle furnace. Thermodynamic data was obtained from the SSUB3 database of Thermo-Calc. A semi-integrated steel mill provided the actual data used, ensuring the results' relevance and validity. The energy and exergy efficiencies found were 92.9% and 90.1%, respectively. Simulations were conducted to examine variations in argon's mass and inlet temperature, as well as electrode active power. The parameters' variations revealed minor impacts on process efficiency, providing insights for effective improvements.

Keywords: Exergy; Refining; Ladle furnace; Steelmaking.

1 Introduction

Exergy analysis is used for optimizing industrial processes, such as secondary refining in steelmaking, aiming to improve efficiency and reduce energy losses. Akiyama et al. [1] identified the relationship between exergy consumption, CO_2 emissions, and steel production through exergy analysis in iron production, aiding in emissions reduction and minimizing exergy consumption. Zanoni et al. [2] emphasize the importance of a structured and methodological approach for the exergy calculation of electric arc furnaces, considering distinct stages for a comprehensive and consistent analysis. Furthermore, the electric arc furnace (EAF) and ladle furnace (LF) exergy analysis conducted by Yetiske et al. [3] revealed a significant exergy loss due to chemical reactions and heat transfer while identifying opportunities for exergy recovery through the utilization of furnace gases.

The history of steel refining has evolved from the smelting and refining of steel through basic and acid open hearth furnaces (OHF) in the 1950s to the use of electric arc furnaces (EAF) and ladle refining furnaces (LRF) in the 1980s, enabling greater efficiency and reduced environmental impact [4,5]. The ladle refining furnace (LRF) is used in the steel industry to refine and adjust the quality of steel produced in steelmaking furnaces, ensuring the removal of impurities and the adjustment of the steel's chemical composition [6].

The LRF container is made of steel and heat-resistant ceramic. It features components such as graphite electrodes to provide electrical energy, an exhaust duct to remove gases, and a chemical injection system to add elements like calcium and aluminum to enhance the steel's quality [7]. The primary purpose of injecting argon gas is to homogenize the metal bath in the ladle refining furnace [8].

Adding ferroalloys and fluxes to the steel in the ladle can affect its temperature, typically resulting in a decrease. However, ferrosilicon is the only ferroalloy that increases the temperature due to the exothermic nature of its dissolution in liquid iron [9].

Refining techniques, including deoxidation, desulfurization, and dephosphorization, ensure the quality and properties of steel by removing impurities and controlling the chemical composition of the metal. These techniques are widely employed in ladle furnaces to refine steel and achieve a high-quality product. The addition of calcium is also studied to modify non-metallic inclusions and improve

[1]Departamento de Engenharia de Materiais, Pontifícia Universidade Católica do Rio de Janeiro, Rio de Janeiro, RJ, Brasil.

*Corresponding author: avillez@puc-rio.br

the machinability of steel, minimizing surface defects related to inclusions and enhancing product quality [1].

Çamdali et al. [10] studied the irreversibility and production cost in the context of ladle furnaces, highlighting the potential for efficiency improvements. They recommended using more efficient refractories to reduce heat losses and increase energy efficiency in this refining stage. In a comprehensive study of ladle furnaces, Çamdali and Tunc [11] employed exergy concepts to understand their operation. The analysis revealed that exergy losses are related to reactions and heat losses to the environment, accounting for approximately 13% of the total.

Min and Jiang [12] investigated the exergy loss in an arc electrode-heated ladle furnace and proposed changes in the slag composition to reduce electrical energy consumption. Using foam slag increased the heating rate and reduced energy consumption per ton of steel. In the study of Yetisken et al. [3,13], an exergy analysis was performed on an integrated ladle furnace system, considering both EAF and LF. The study highlighted the significant usage of argon, resulting in higher expenses, and emphasized the importance of optimizing the consumption of this input to reduce operational costs.

The present study developed a program to apply exergy concepts to assess the performance of a ladle furnace in a steelmaking plant, identify improvements, and suggest how to improve the process. A brief introduction to exergy will be presented, followed by the program organization, and its application to the ladle furnace.

2 Exergy

The exergy approach includes the thermodynamic system with its modified neighborhood, the nearest environment, where all the heat, reactions, and mass transfers occur. Outside this region, the local environment is in thermodynamic equilibrium without gradients in its properties and with constant composition. Only work is exchanged between the local environment and the exergetic system. According to Kotas et al. [14], the system's interaction with the environment can affect energy availability, rendering some forms of work unusable for application.

The concept of thermodynamic equilibrium is essential in the energy analysis of systems, as it allows quantifying exergy, which is the energy available to be converted into work. The maximum work a system performs occurs during the interaction between the system and the environment until the system reaches the state of equilibrium. No work is produced in the equilibrium state, known as the dead state. This thermodynamic analysis considers the parameters required to achieve equilibrium in a small region, including the system and immediate surroundings.

The immediate surroundings refer to everything not included in the system but that may be affected by the system [15]. The environment is a portion of the surroundings

away from the system such that the intensive properties of each phase are uniform and do not change significantly due to any process inside the system. The boundary between the environment and the system is defined as adiabatic. Figure 1 schematically illustrates the system boundary, demarcating the system, constituted by the thermodynamic system and its immediate surroundings, and the surrounding boundary, encompassing the system within an invariant environment.

Exergy can be expressed by four main components: kinetic exergy (Exk), potential exergy (Exp), physical or thermomechanical exergy (Exph), and chemical exergy (Exch), as shown in Equation 1. Each of these components is relevant in identifying opportunities for improving the energy performance of a system, as it allows us to identify energy flows that can be converted into useful work [16].

$$Ex = Ex_{ph} + Ex_{ch} + Ex_p + Ex_k \qquad (1)$$

Physical exergy is the portion of exergy that relates to the thermodynamic properties of a system with respect to reference conditions, such as temperature and pressure. It is quantified by the Equation 2 that expresses the difference between the system's enthalpy and entropy and the reference conditions. As shown in Equation 2, physical exergy identifies the work potential of a system, and it is applied in energy analysis to increase the efficiency of processes and systems [6,17].

$$Ex_{ph} = (H - H_0) - T_f (S - S_0) \qquad (2)$$

According to Dunbar et al. [18], the kinetic and potential exergy of a fluid changes as it moves with an average mass velocity due to various factors such as exergy liquid transport, work done on the fluid, reversible interconversion with deformation exergy, potential variations in exergy, and irreversible conversions that transform energy into heat. The potential energy Equation 3 is calculated as the product of gravity (g), height (z), and mass (m). The kinetic energy Equation 4 describes the amount of energy a bubbling gas transfers to a metal bath. It is calculated by the gas flow rate (V), temperature of the metal bath (T), tonnage of mass in the bath (M), depth of gas injection (H), and pressure at the surface of the metal bath (P) [19].

$$Ex_p = Mgz \qquad (3)$$

$$Ex_k = 14,23 * \left(\frac{VT}{M}\right) log\left(\frac{1+H}{1,48P}\right) \qquad (4)$$

In addition, we can mention electrical exergy, which is another measure of the available exergy in an electrical system, indicating its capacity to perform useful work. It is determined by integrating electrical power, P, over time according to the Equation 5 [20]:
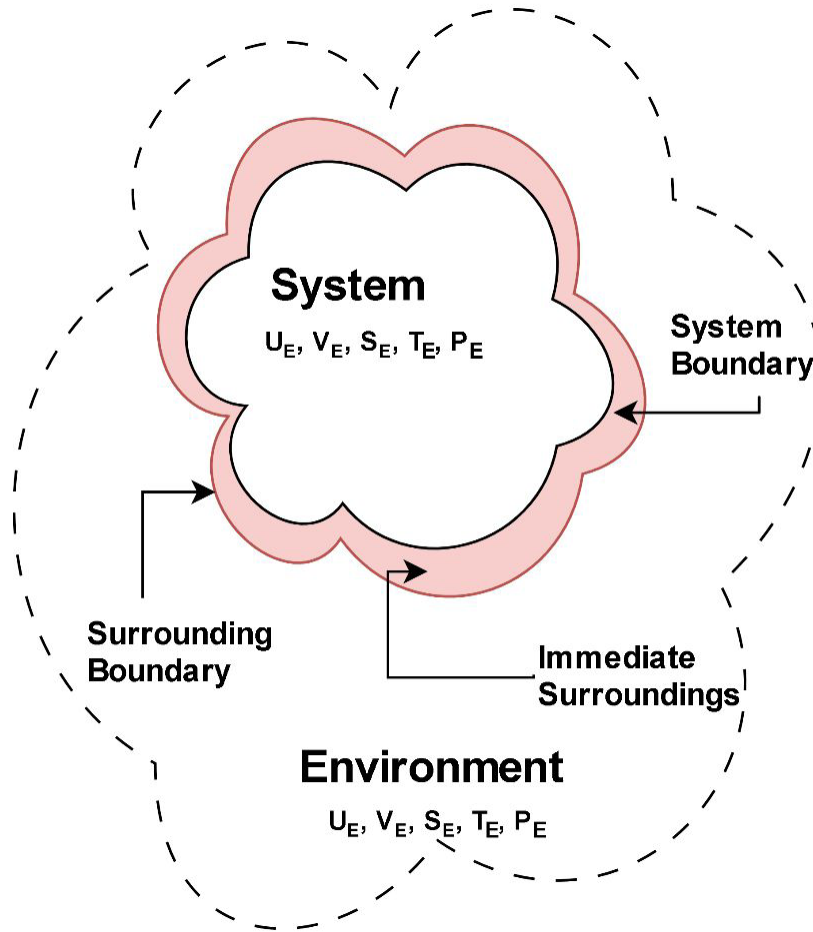
Figure 1. Interaction of the system with the environment.

$$Ex_p = \int_{t_0}^{t_f} P\,dt \qquad (5)$$

The exergy of a system is described through an exergy balance, where the amount of exergy entering the system (Ex_e) equals the amount leaving the system (Ex_l) plus the amount of exergy loss (Ex_d) during the process according to the Equation 6 [16]:

$$Ex_e = Ex_l + Ex_d \qquad (6)$$

According to Ramakrishna et al. [21], exergetic efficiency, Equation 7, is a measure defined as the ratio of the exergy of the product of interest to the sum of the input exergies in the process. This measure considers the energy quality involved and assesses the potential for useful work in the process.

$$Exf = \frac{M_{out\_st} Ex_{out\_st}}{\sum M_{in} Ex_{in}} \qquad (7)$$

M_{out_st} and Ex_{out_st} represent the mass and exergy of liquid steel at the outlet. M_{in} and Ex_{in} correspond to the mass

and exergy of all input streams. Similarly, we calculate the efficiency of the steel input converted into products using Equation 8:

$$Ef = \frac{M_{out\_st} E_{out\_st}}{\sum M_{in} E_{in}} \qquad (8)$$

M_{out_st} and E_{out_st} represent the mass and energy of liquid steel at the outlet. M_{in} and E_{in} correspond to the mass and energy of all input streams.

2.1 Exergy analysis procedure

A Python program using a Jupyter Notebook was developed to analyze processes' energy and exergy. The program's inputs are mass and energy currents, which describe the system's input and can have their values increased or reduced depending on the system's details. The program's output presents the energy and exergy results in each chain for the global results. So, the program can be applied to any industrial process. The current study case is the ladle refining furnace. Figure 2 presents a flowchart illustrating the proposed algorithm.
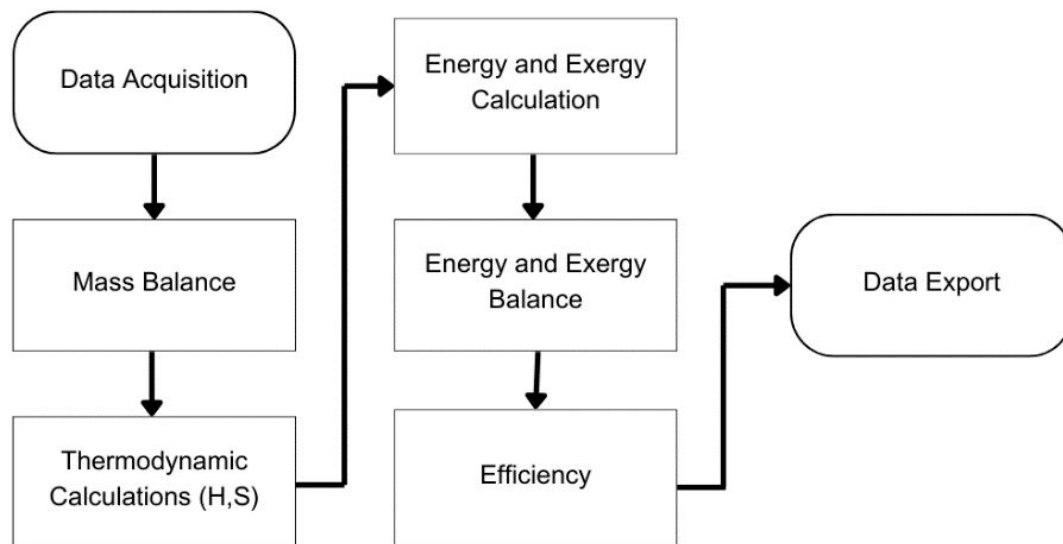
Figure 2. Program's flowchart

Data collection and organization followed a detailed process with clearly defined stages. Initially, the necessary data were obtained from a steel industry company, compiled, and organized in Excel format. Next, these data were imported into the Python programming environment to facilitate analysis and subsequent processing by creating a dataframe, as presented in Tables S12–S21. This transition allowed the efficient execution of subsequent calculations and analyses, providing a cohesive structure to the dataset.

A starting point throughout the program development, highlighted in the supplementary material, involved invoking and utilizing specific libraries dedicated to dataframe manipulation, mathematical operations, and graphical visualization. Incorporating these libraries laid the foundations for code structuring and enabled the effective implementation of the program's essential functionalities, thereby consolidating its robustness and operational flexibility.

The use of the Pandas library (https://pandas.pydata.org/) in the context of this article stands out for its remarkable effectiveness in data manipulation and analysis, providing efficient management of datasets. The NumPy library (https://numpy.org/), specialized in array manipulation and numerical calculations, is used to optimizing mathematical operations within the Python environment. The enhancement of numerical integration functionality is notable with the presence of the SciPy library (https://scipy.org/), particularly through the 'quad' function, significantly expanding the code's capabilities and making it more robust for advanced scientific calculations. In the visualization realm, the efficiency provided by the Matplotlib library (https://matplotlib.org/) is noteworthy, enabling the creation of informative graphs that enhance the visual representation of results. The contributions of the mentioned libraries not only improve the code's functionality but also enrich the analysis and interpretation of data in the context of this study.

All substances' enthalpy and entropy were calculated using the SSUB3 database and the Thermo-Calc software (version 2015). The program takes a dataframe containing the real data subject to analysis as input, along with a series of text files in '.txt' format containing the individual thermodynamic values of each component involved. For each process, an appropriate thermodynamic database should be applied.

An interpolating function was implemented as an integral part of the program to provide the enthalpy and entropy values to the dataframe, considering the individual enthalpy and entropy values per mole for each stream. This function associates the thermodynamic values at the right temperature to each component in every stream.

In the program, the dissociation energy of the molecules in the ladle furnace's metal bath was disregarded to simplify the thermodynamic calculation. The thermodynamic data, enthalpy, and entropy for reactions with the oxygen dissolved in the steel were corrected for the oxygen dissolution in iron, as per Equation 9, before being input into the program [17].

$$\Delta G(T) = -115750 - 4.63 T J / molO \qquad (9)$$

Before the mass and energy balance, the program allows the adjustments of the input variables, aiming to assess and enhance the process. The initial temperature of argon, the slag composition, the liquid iron mass, the argon's total mass, and the electrode active power are critical variables. This flexibility in customizing input variables enables a comprehensive analysis of various operational conditions, allowing the program to adapt to the specific needs of the process. Pure iron's properties were used for the liquid iron alloy's thermodynamic properties. However, the thermodynamic reactions with ferroalloys and alloying elements were evaluated since these reactions may result in substantial energy and exergy changes.

In the subsequent stage, during the balance calculations, masses from each stream are aggregated to perform the mass balance. This analysis estimates the difference between the input and output masses, offering a precise assessment of mass variations in the system, as outlined in Equation 10. This process is useful for a comprehensive understanding of interactions and mass flows within the system, contributing to an efficient and informed management of the process at hand.

$$M_b = \sum M_{out} - \sum M_{in} \qquad (10)$$

An individual table is generated for each stream, displaying mass values (kg) for each component. Additionally, a comparative graph is constructed to provide a clear visualization of output and input masses, highlighting the resulting representation of the balance.

This graphical approach enables immediate visual analysis and a more intuitive understanding of mass variations in the system, making any imbalances or relevant patterns evident during the process analysis.

After the mass balance, the components' mass is converted to mol for each stream according to Equation 11. N represents the number of moles, M is the component's mass, and MM is its molar mass.

$$N = \frac{M}{MM} \qquad (11)$$

Next, an energy balance is performed analogously to the mass balance according to Equation 12. This equation balances enthalpies by subtracting the input and reaction enthalpies from the output enthalpy. Specific tables are generated for each stream, presenting relevant energy values. Additionally, a graph is constructed to illustrate and compare energy variations highlighting the energetic dynamics throughout the process.

$$E_b = \sum E_{out} - \sum E_{in} \qquad (12)$$

Subsequently, a function specifically designed for entropy calculation is activated. This function performs entropy calculations considering the mole quantity of each component in the system. Additionally, a dedicated function was developed to calculate the entropy of mixing. The program calculates the exhaust gas and the slag entropies of mixing, as detailed in Equation 13. The mixing process increases the entropy of the system and, therefore, changes the exergy.

$$S = \sum_i -8.314 . N_i . ln\left(\frac{N_i}{\sum N_i}\right) \qquad (13)$$

The chemical exergy of each reaction was calculated using the data provided by Szargut [22] for the involved elements and compounds. These values were subsequently integrated into Equation 2.

Following the entropy calculations, physical and kinetic exergies were determined, representing a step in assessing the availability of work and the quality of various forms of energy in the system. The exergy balance was conducted using Equation 14. The corresponding exergies were then incorporated into relevant specific tables, and subsequently, comparative graphs were generated, following a similar approach to the process carried out for energy and masses.

$$Ex_b = \sum Ex_{out} - \sum Ex_{in} \qquad (14)$$

After calculating enthalpy, entropy, and exergy, Equation 8 and 9 calculated the system's exergy and energy efficiency. This measure is essential for evaluating the process's performance and providing information about the efficiency in energy conversion and resource utilization. The results were stored in a new dataframe, which consolidated all the information gathered during the analysis. This approach provided a clear and organized data visualization, facilitating interpretation and decision-making related to the studied process.

Based on the collected data and the information stored in the dataframe, simulations were conducted to evaluate improvements and changing parameters in the process. Various scenarios and strategies were explored by manipulating the parameters and variables to maximize energy efficiency, minimize losses, and improve product quality.

The mass and thermodynamic data presented by Çamdali and Tunc [11] were used as a test to validate the accuracy and quality of the program, facilitating a more complete evaluation of the results. After this verification, an exergy analysis was performed with data provided by a siderurgy company and the mass, energy and exergy balances were analyzed.

3 Exergy analysis results and discussions

Tables (S1) to (S11) present the input and output streams for refining 1010 steel in a ladle furnace. Mass components from other streams. The thermodynamic properties for this stream were calculated using the reaction enthalpy values evaluated at the temperature of the metal bath (1893.15 K). This temperature was measured after the liquid metal from the EAF equilibrates in the LF. It is important to emphasize that, for the P_2O_5 component, we used data reported in the literature [23] due to the limitations of the employed database, which only includes thermodynamic data tabulated up to 1080 K. The compounds N_2, B, V_2O_5, S, P, and N_2 were not included in the present study.

The program Thermo-Calc does not directly calculate exergy, as it depends on the ambient temperature T_f as defined in Equation 2. The solution energy was obtained as the weighted sum of enthalpies and the ideal mixing entropy, without considering the non-ideal mixing enthalpy.

The argon gas kinetic exergy was determined using Equation 4, which considers the effects related to the velocity of the components. The calculation resulted in a kinetic

energy of 40.9 kJ; a small value compared to the magnitude of the exergy of the other streams.

The chemical exergy was 96800 kJ. The multiplication of the enthalpy and entropy per mole of each component by the corresponding number of moles was performed for evaluation. Thermodynamic data for enthalpy, entropy, and exergy are detailed in Tables 1 to 6. Some enthalpy values show a positive sign in the formation of oxides, as these compounds are decomposing in the furnace instead of being formed.

Table 7 presents each stream's total mass, energy, and exergy. As expected, the mass of the input and output steel streams controls the energy and exergy balance due to their mass. The mass balance required an adjustment. The output streams' exact values are unknown, so a 200 kg difference between the input and output masses was found

Table 1. Slag from FEA thermodynamic data at 1887.15 K

Composition	Enthalpy (J)	Entropy (J/K)	Exergy (J)
Al_2O_3	9.67E+07	1.02E+05	6.62E+07
CaO	8.97E+08	1.02E+06	5.94E+08
Cr_2O_3	4.83E+06	5.46E+03	3.20E+06
FeO	7.84E+08	8.71E+05	5.25E+08
MgO	3.55E+08	3.95E+05	2.37E+08
MnO	7.93E+07	8.81E+04	5.30E+07
P_2O_5	1.14E+06	0.00E+00	0.00E+00
SiO_2	7.69E+08	8.42E+05	5.18E+08
TiO_2	4.30E+06	4.75E+03	2.88E+06
CaF_2	1.54E+07	1.47E+04	1.10E+07

Table 2. Liquid iron thermodynamic data at 1887.15 K

Composition	Enthalpy (J)	Entropy (J/K)	Exergy (J)
C	1.45E+08	1.50E+05	1.01E+08
Mn	6.14E+07	6.02E+04	4.34E+07
Si	1.59E+07	1.32E+04	1.20E+07
Cu	1.28E+08	1.32E+05	8.84E+07
Cr	8.72E+07	9.13E+04	5.99E+07
Ni	8.09E+07	7.89E+04	5.74E+07
Mo	2.82E+06	3.13E+03	1.89E+06
Sn	7.29E+06	9.33E+03	4.51E+06
Nb	2.38E+06	2.67E+03	1.58E+06
V	9.49E+05	1.04E+03	6.41E+05
Fe	1.06E+11	1.14E+08	7.16E+10

Table 3. Exhaust gas thermodynamic data at 1893.15 K

Composition	Enthalpy (J)	Entropy (J/K)	Exergy (J)
Ar	1.04E+09	1.20E+06	6.78E+08
CO	2.56E+08	2.84E+05	1.72E+08

Table 4. Output slag thermodynamic data at 1893.15 K

Composition	Enthalpy (J)	Entropy (J/K)	Exergy (J)
Al_2O_3	1.25E+08	1.33E+05	8.52E+07
CaO	2.20E+09	2.47E+06	1.46E+09
Cr_2O_3	1.10E+07	1.23E+04	7.28E+06
FeO	2.26E+08	2.50E+05	1.51E+08
MgO	6.66E+08	7.38E+05	4.46E+08
MnO	1.83E+07	2.05E+04	1.22E+07
SiO_2	1.28E+09	1.39E+06	8.60E+08
TiO_2	7.95E+06	8.72E+03	5.35E+06
CaF_2	5.90E+06	5.68E+03	4.21E+06

Table 5. Refined steel thermodynamic data at 1893.15 K

Composition	Enthalpy (J)	Entropy (J/K)	Exergy (J)
C	2.83E+08	2.90E+05	1.97E+08
Mn	6.51E+08	6.36E+05	4.62E+08
Si	3.49E+08	2.88E+05	2.63E+08
Cu	1.29E+08	1.33E+05	8.93E+07
Cr	9.00E+07	9.36E+04	6.21E+07
Ni	8.17E+07	7.93E+04	5.80E+07
Mo	2.85E+06	3.15E+03	1.92E+06
Sn	7.35E+06	9.37E+03	4.56E+06
Nb	2.41E+06	2.68E+03	1.61E+06
V	9.62E+05	1.04E+03	6.51E+05
Fe	1.07E+11	1.15E+08	7.30E+10

Table 6. Reaction thermodynamic data at 1893.15 K

Reaction	Enthalpy (J)	Entropy (J/K)	Exergy (J)
$2Al + 3/2\ O_2 \rightarrow Al_2O_3$	-1.12E+08	-2.60E+04	-1.04E+08
$2P + 5/2\ O_2 \rightarrow P_2O_5$	-1.39E+08	-5.23E+04	-1.23E+08
$C + 1/2\ O_2 \rightarrow CO$	-1.11E+07	4.27E+05	-1.38E+08
$Mn + 1/2\ O_2 \rightarrow MnO$	-2.07E+08	-5.98E+04	-1.90E+08
$Si + O_2 \rightarrow SiO_2$	-2.63E+09	-6.92E+05	-2.42E+09
$Fe + 1/2\ O_2 \rightarrow FeO$	-8.00E+08	-2.67E+05	-7.20E+08

Table 7. Data on the sums of mass, energy, and exergy.

Stream	Mass (kg)	Energy (J)	Exergy (J)	Temperature In/ Out (K)
Argon	1247	0.00E+00	0.00+04	298.15
Cold slag	1136	0.00E+00	0.00E+00	298.15
FEA slag	1977	3.01E+09	2.01E+09	1887.15
Additional elements	146	0.00E+00	0.00E+00	298.15
Ferroalloys	781	0.00E+00	0.00E+00	298.15
Liquid iron	97831	1.06E+11	7.19E+10	1887.15
Electrode active power	20	6.48E+09	6.48E+09	298.15
Exhaust gas	1499	1.29E+09	8.49E+08	1893.15
Output slag	2782	4.53E+09	3.03E+09	1893.15
Refined steel	98860	1.09E+11	7.42E+10	1893.15
Reaction	0	1.60E+09	1.86E+09	1893.15

and adjusted in the output stream. The slag mass balance elements were also adjusted to obtain adequate closure.

The ladle sealing sand is Cr_2O_3 based, therefore, an amount of chromium oxide was considered in the cold slag. Sand fills the FEA valve channel. When the drawer is open, the sand is carried with the liquid steel.

After carefully analyzing the streams involved in the process and considering the quantity of each element present, it was decided to correct the difference in the input liquid steel, thus ensuring that the iron in the system was correctly balanced.

The stream's energies and exergies were calculated considering this correction. The electrode active power and exergy are about 6% and 9% of the input steel's energy and exergy, respectively; however, the exhaust gas gains appreciable energy and exergy from interacting with the liquid steel.

Table 8 shows the net values of energy and exergy and their balances. The steelmaking system's exergy and energy efficiencies were calculated using Equations 8 and 9, respectively. The remarkable results indicate an energy efficiency of 92.9% and an exergy efficiency of 90.1%.

Figure 3 depicts the energy and exergy balance obtained. It shows the input, output, reaction streams, and balance, which is the difference between the initial and final values of energy and exergy.

In Figure 3, most energy and exergy correspond to the molten steel at the inlet and refined steel at the outlet. The increase in energy and exergy of the refined steel compared with the equilibrated molten steel relates to a temperature

Table 8. Enthalpy, entropy, and exergy balance.

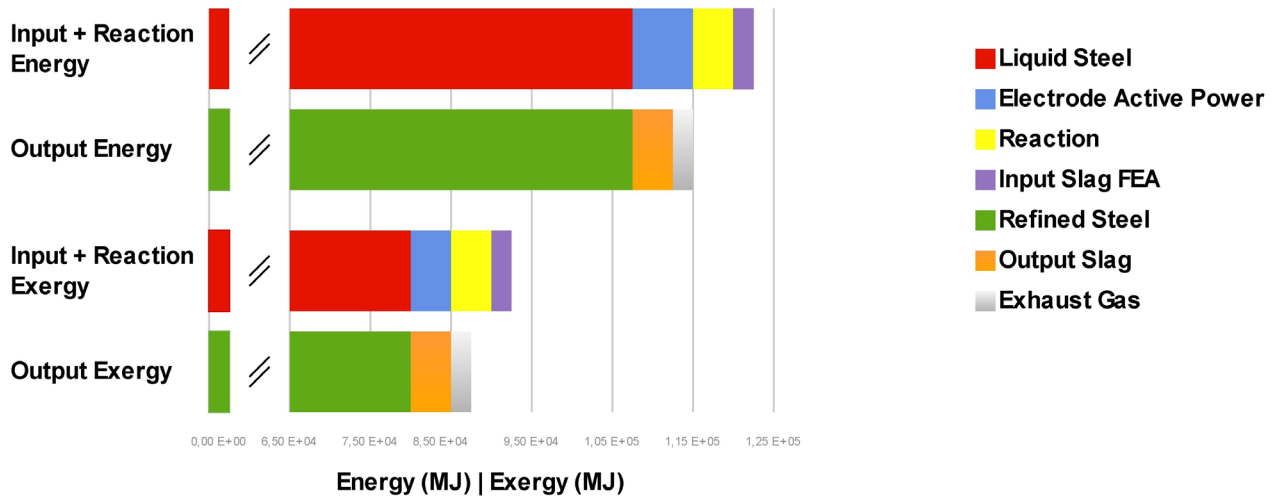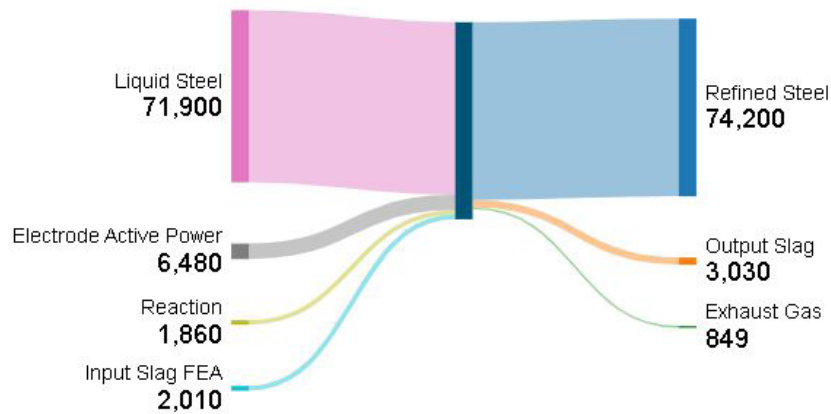| Stream	Mass (kg)	Energy (J)	Exergy (J)
Input	103142.1	1.09E+11	7.40E+10
Electrode	0	6.48E+09	6.48E+09
Reaction	0	1.60E+09	1.86E+09
Output	103142.1	1.15E+11	7.80E+10
Balance	0.001	-2.39E+09	-4.26E+09

Figure 3. Energy and Exergy balance.

Figure 4. Sankey diagram

increase of 16°C from the initial molten iron temperature in the LF. The exhaust gas and slag streams from the LF carry a significant exergy. It is worth noting that the heat from these streams is not utilized for other processes in the ladle furnace under study. In this sense, the exhaust gases could be used to heat inlet streams in the process. The Sankey diagram in Figure 4 was constructed to illustrate the exergy flow shifts from the input to the output stream.

Temperature loss from the LF was 1 °C to 3 °C per minute, and the total process took 48 minutes. So, the program could estimate the minimum and maximum energy and exergy losses. The minimum energy and exergy losses were 3% and 4% for a 1°C/min temperature reduction, and the maximum losses were 12% and 14% for a 3°C/min temperature reduction. These values are consistent with the program's calculated energy and exergy efficiencies.

Analyzing the work of Çamdali et al. [10] for a 55 ton ladle furnace allows us to deduce that the energy lost through thermal exchanges is approximately 3%. Their value is consistent with the estimated values in the current work. Additionally, the total energy used for refining steel was around 87%, a value close to the energy efficiency found in the present work, which is 92.9%. Both studies do not account for the temperature loss when pouring the molten steel from the EAF to the ladle furnace. On the other hand, the exergetic efficiency found in Çamdali´s work (50%) was very different from the present work (90.1%). It is important to notice that Çamdali et al. [10] considered the liquid temperature in the EAF before equilibrating with the ladle furnace, and the present study considers the ladle temperature after a short equilibration time.

Comparing the results obtained with the data available in Çamdali's paper [11] to the information in the current work, we observe a consistency in the order of magnitude of the analyzed variables. When analyzing the gases, for instance, we note that the enthalpies of argon and exhaust gas are of the same order of magnitude as the values found in the work. Although the exergetic efficiency value (81%) differs from that found in the current work (92.9%), it was indicated that the total exergetic loss by the ladle furnace is 13%, a value close to the calculated losses in the current work (4 to 14%).

The refractory material is in direct contact with the metallic bath and the slag; in the outermost layer, the thermal insulating material surrounds the refractory. Both refractory and insulation are oxides, however, the insulation material is a very porous oxide to improve insulation.

Min and Jiang [12] analyzed a ladle furnace with a capacity of 150 tons of steel. The calculated exergy efficiency was 98.27%, considering the energy of refined steel and slag leaving the FEA. However, this efficiency is very high and may not be in line with reality. The surprising difference found in efficiency of Min and Jiang [12] and Çamdali et al. [10] could be a result of the quality of the materials used to insulate the ladle oven.

Although the articles do not describe it precisely, high efficiency values may be related to the fact that the process inlet temperature is assumed to be that of the steel and slag when they enter the ladle furnace in a liquid state. Furthermore, the heat lost when transferring the contents of the EAF to the ladle furnace is not considered.

4 The effect of some process parameters on the energy and exergy.

Although Çamdali and Tunç [11] data was used to verify the present program, their research lacks detailed information on stream compositions and specific thermodynamic data, so it represents a significant obstacle to the effective use of their study. This essential data is necessary to a comprehensive understanding of the influential variables in the process.

Min and Jiang's [12] initial analysis of the ladle furnace energy losses revealed considerable dissipation, mostly associated with unavailable electrical energy, accounting for approximately 56.98% of the total exergy losses. Min and Jiang [12] proposed the submersion of the electrode in the foaming slag with notable improvements in the system's performance. Optimized industrial experiments indicated a reduction of 21,730MJ of unavailable electrical energy per ton of steel and a 14.84% increase in the exergetic efficiency of electrical energy. These results highlight the effectiveness of specific strategies to mitigate energy losses in the ladle furnace.

The study conducted by Min and Jiang [12], through changing parameters tests, represents a significant contribution to understanding the ladle furnace. However, it is worth noting that, despite addressing variations in the carbon electrode's immersion height and slag composition, certain critical factors were neglected. Their evaluation did not include the variation in electrical energy supplied to the electrode, the temperature of liquid iron at the input, the argon temperature, and its mass at the process. These elements play crucial roles in the ladle furnace's performance, and their exclusion emphasizes specific areas that our study aims to encompass and fully understand.

The present study varied one process parameter while keeping all the others identical to the values informed by the steel company. Variation of the electrical energy supplied by the electrodes presented in Table 9 showed a marked influence on the energy and exergy efficiencies. So, electrode active power must be carefully considered in the process. The simulations were carried out with the bath at a temperature of 1893.15K.

Çamdali et al. [10] showed that the available work increases as the temperature of the liquid steel rises. Therefore, removing the steel at the appropriate temperature could be an opportunity for improvement. However, the ladle furnace is a refining furnace. From this perspective, the appropriate exit temperature in the present work was not altered to avoid any issues related to the steel quality.

The proposal to explore ways to enhance energy efficiency without compromising the bath temperature is strategic and aligns with essential economic goals.

Table 9. Efficiency achieved as a function of supplied active electric power

Electric power (J)	Energy efficiency (%)	Exergy efficiency (%)
4.50E+09	94.5	92.3
5.00E+09	94.2	91.7
5.50E+09	93.7	91.2
6.00E+09	93.4	90.6
6.48E+09	92.9	90.1
7.00E+09	92.6	89.5
7.50E+09	92.2	89.0
8.00E+09	91.8	88.5
8.50E+09	91.4	87.9

Table 10. Efficiency achieved as a function of the inlet metallic bath temperature

Temperature (K)	Energy efficiency (%)	Exergy efficiency (%)
1847.15	95.0	92.4
1857.15	94.3	91.7
1867.15	93.6	90.8
1877.15	92.9	90.1
1887.15	92.3	89.4
1897.15	91.7	88.6
1907.15	91.0	87.8

Table 11. Efficiency achieved as a function of the input argon temperature

Temperature (K)	Energy efficiency (%)	Exergy efficiency (%)
298,15	92.9	90.1
500.15	92.8	90.0
700.15	92.7	90.0
900.15	92.6	89.9
1100.15	92.5	89.8
1300.15	92.4	89.7
1500.15	92.3	89.6

Table 10 presents the possibility of working with slightly different temperatures to achieve substantial energy savings, directly contributing to cost reduction per heat. When applied over multiple heats, this approach can positively impact the company's profit, representing an effective strategy for decreasing operational expenses.

The current study confirms that the available exergy and energy efficiency decrease with the temperature of the liquid steel entering the ladle furnace. Table 10 shows the temperature variation of the metallic bath. The electrode active power was constant and equal to 6,48.109J. The inlet temperature of the molten steel in a typical run is 1877.15K for the present study.

The similarity between the energy and exergy efficiencies observed in this study is attributed to the absence of temperature loss considerations during the transfer of liquid steel from the EAF to the ladle furnace. If this thermal loss were accounted for, the exergy variation would be significantly higher, leading to a more pronounced discrepancy between the efficiencies.

It can be noted that efficiency increases when the input temperature of molten iron and slag in the system is reduced. However, as previously discussed regarding the electrode, it is understood that, despite being a variable, the steel production temperature must be adequate to maintain its quality.

Furthermore, this work did not consider the thermal losses from transferring steel and slag from the EAF to the ladle furnace (LF). The input temperature is the temperature measured in the LF after equilibration with the furnace, so it is smaller than the tapping temperature. This discussion raises the hypothesis of trying to reduce transfer losses. Steel is poured from the EAF in just two minutes. During this time, the stream loses up to 50 °C due to radiation and conduction during equilibration with the furnace.

Argon is an important inert gas in the steelmaking process. It homogenizes the metal bath's composition and temperature, ensuring stable and controlled conditions in the ladle furnace. Changes in the mass and temperature of argon gas must be carefully evaluated to prevent the compromise of homogenizing function.

In energy and exergy analysis, the variation in argon's inlet mass is insignificant when maintaining a temperature of 298.15 K. This is because this temperature was chosen as the reference standard, making the enthalpies and exergies at this temperature zero.

Adjusting the argon inlet temperature, without modifying its mass, could offer a strategic opportunity to enhance the efficiency of the steelmaking process, but the impact is small, as indicated in Table 11. In this simulation, the mass of argon used was 1247 kg.

The variations are too small to be considered and similar to the efficiency variations of about 1% of the total value found by Çamdali et al. [10] for exhaust gas temperature. It should also be noted that argon agitation is favored due to the gas expansion that occurs when its temperature increases. So, changes in inlet temperature need to be carefully evaluated, as they can harm the homogenization of the metal bath. However, the effluent gases, argon, and CO_2, carry considerable thermal energy which may be used heating another process in the industry by energy integration.

An additional proposal to improve the overall energy and the exergy efficiency is to implement heat exchanges between streams that would otherwise be discharged into the atmosphere. Slag, steel exposed to the atmosphere for cooling, and exhaust gas represent significant thermal streams that can be leveraged for energy recovery. Indeed, gas streams are relatively simpler to apply in heat exchanges, and the exhaust gas amount increases with 135 kg of CO per batch, according to the present estimates, which reacts with the oxygen from the infiltrated air. This exhaust gas is at a very high temperature and may be used in heat exchangers after being cleaned from the dust.

Heat transfer efficiency and minimizing losses are crucial in steel production, especially during the transference of liquid metal from the electric arc furnace (EAF) to the ladle furnace. Currently, there are no effective mechanisms in the plant studied to prevent heat loss during this process. When steel is poured from the EAF to the ladle furnace, significant heat transfer occurs due to the temperature difference between the two environments.

This heat loss can result in a decrease in the temperature of the liquid metal, impacting the quality of the steel produced and increasing the need to reheat the metal, which in turn consumes more energy.

Furthermore, an economic return analysis using thermodynamic and economic concepts can be developed to estimate costs, as was done by Yetisken et al. [13] when analyzing the LF and EAF. This study did not examine the dust leaving the furnace with the exhaust gases. It is recommended that the thermodynamic influence of dust be evaluated in future work. Exploring opportunities for utilizing slag and exhaust gases, such as carbon monoxide, is also a proposal for future work.

5 Conclusions

A program was developed in Python using Jupyter Notebook to study the energy and exergy efficiencies of chemical and metallurgical processes. The program considers the mass, energy and exergy streams in and out the system of interest. So, it may be easily applied to any metallurgical or chemical process.

The energy and exergy efficiencies for the studied ladle refining furnace were 92.9% and 90.1%, respectively. These values are reasonably high compared to other efficiencies in the literature but consistent with the present furnace's thermal losses.

The kinetic exergy of gases and chemical exergy of the liquid mixture values were 40.9 kJ e 96800 kJ, respectively. These values are very small compared to the energy values of each major stream entering or leaving the ladle furnace.

The effect of some process parameters on the energy and exergy efficiencies was evaluated. Reducing the active electrode power stands out. The less energy the electrode consumes, the more efficient the process becomes. The liquid bath's inlet temperature impacts energy and exergy efficiency. However, small changes in the argon inlet temperatures do not significantly change the energy and exergy values.

Acknowledgements

References

1 Akiyama T, Yagl JI. Methodology emission and to evaluate reduction limit of minimum exergy consumption carbon dioxide tor lronmaking. J International. 1998;38(8):896-903.

2 Zanoni C, Kaehler W. Análise exergética de um forno elétrico a arco. Porto Alegre: Pontifícia Universidade Católica do Rio Grande do Sul; 2004.

3 Yetisken Y, Çamdali U, Ekmekci I. Optimum charging materials for electric arc furnace (EAF) and Ladle Furnace (LF) System: a sample case. Jestech. 2012;15(2):77-83.

4 Sahoo PK. Exergoeconomic analysis and optimization of a cogeneration system using evolutionary programming. Applied Thermal Engineering. 2008;28(13):1580-1588.

5 Zhang P, Jin Q. Evolution, status, and trends of exergy research: a systematic analysis during 1997–2020. Environmental Science and Pollution Research International. 2022;29(49):73769-73794.

6 Behzadi A, Houshfar E, Gholamian E, Ashjaee M, Habibollahzade A. Multi-criteria optimization and comparative performance analysis of a power plant fed by municipal solid waste using a gasifier or digester. Energy Conversion and Management. 2018;171:863-878.

7 Sheng J, Voldsund M, Ertesvåg IS. Advanced exergy analysis of the oil and gas processing plant on an offshore platform: a thermodynamic cycle approach. Energy Reports. 2023;9:820-832.

8 Bai J, Tu C, Bai J. Measuring and decomposing Beijing's energy performance: an energy- and exergy-based perspective. Environment, Development and Sustainability. 2024; **26:**17617-17633.

9 Macedo Costa M, Schaeffer R, Worrell E. Exergy accounting of energy and materials flows in steel production systems. Energy. 2001;26:363-384.

10 Çamdali U, Murat T, Feridun D. A thermodynamic analysis of a steel production step carried out in the ladle furnace. Applied Thermal Engineering. 2001;21:643-655.

11 Çamdali U, Tunc M. Energy and exergy analysis of a ladle furnace. Canadian Metallurgical Quarterly. 2003;42(4):439-446.

12 Min Y, Jiang MF. Exergy analysis and optimization of ladle furnace refining process. Journal of Iron and Steel Research International. 2010;17:24-28.

13 Yetisken Y, Çamdali U, Ekmekci I. Cost and exergy analysis for optimization of charging materials for steelmaking in eaf and lf as a system. Metallurgist. 2013;57(5):1133-1140.

14 Kotas TJ, Boston L, Singapore D, Wellington ST. The exergy method of thermal plant analysis. London: Anchor Brendon Ltd; 1985.

15 Moran MJ, Sciubba E. Exergy analysis: Principles and practice. Journal of Engineering for Gas Turbines and Power. 1994;116(2):285-290.

16 Ebrahimi A, Houshfar E. Thermodynamic analysis and optimization of the integrated system of pyrolysis and anaerobic digestion. Process Safety and Environmental Protection. 2022;164:582-594.

17 Turkdogan EJ, Fruehan RJ. Fundamentals of iron and steelmaking. In: Fruhen RJ, editor. The making, shaping and treating of steel, 11th ed. Pitsburgo: United States Steel Corp; 1998, p. 92.

18 Dunbar WR, Lior N, Gaggioii RA. The component equations of energy and exergy. Journal of Energy Resources Technology, Transactions of the ASME. 1992;114(1):75-83.

19 Kor GJW, Glaws PC. Ladle refining and vacuum degassing. In: Fruhen RJ, editor. The making, shaping and treating of steel. 11th ed. Pitsburgo: United States Steel Corp; 1998, p. 669.

20 Terzi R. Application of exergy analysis to energy systems. In: Tner T, editor. Application of exergy. London: InTech; 2018; p. 109-123.

21 Ramakrishna G, Kadrolkar A, Srikakulapu NG. Exergy and its efficiency calculations in ferrochrome production. Metallurgical and Materials Transactions. B, Process Metallurgy and Materials Processing Science. 2015;46(2):1073-1081.

22 Szargut J. Chemical exergies of the elements. Applied Energy. 1989;32:269-268.

23 Jung IH, Hudon P. Thermodynamic assessment of P 2O 5. Journal of the American Ceramic Society. 2012;95(11):3665-3672.

Supplementary Material

Supplementary material accompanies this paper.

Table S1: Argon input data.
Table S2: Slag input data from FEA.
Table S3: Cold additional slag input data.
Table S4: Refined steel input data.
Table S5: Iron alloy input data.
Table S6: Input data for additional elements.
Table S7: Electrode mass loss input data.
Table S8: Exhaust gas output data.
Table S9: Slag Output Data.
Table S10: Refined steel output data.
Table S11: Reaction data.
Table S12: Argon thermodynamic data at 298.15 K
Table S13: slag from FEA thermodynamic data at 298.15 K
Table S14: Cold slag thermodynamic data at 298.15 K.
Table S15: Liquid iron thermodynamic data at 298.15 K.
Table S16: Thermodynamic data of ferroalloys at 298.15 K.
Table S17: Thermodynamic data of additional elements at 298.15 K
Table S18: Electrode thermodynamic data at 298.15 K
Table S19: Exhaust gas thermodynamic data at 298.15 K
Table S20: Output slag thermodynamic data at 298.15 K
Table S21: Refined steel thermodynamic data at 298.15 K

This material is available as part of the online article from https://doi.org/10.4322/2176-1523.20253159